

## Electronic Supplementary Information (ESI)

*for*

### **Polydopamine-embedded $\text{Cu}_{2-x}\text{Se}$ nanoparticles as sensitive biosensing platform through the coupling of nanometal surface energy transfer and photo-induced electron transfer †**

Hong Yan Zou,<sup>ab</sup> Peng Fei Gao,<sup>a</sup> Ming Xuan Gao<sup>b</sup> and Cheng Zhi Huang<sup>\*ab</sup>,

<sup>a</sup> *Key Laboratory of Luminescence and Real-Time Analytical Chemistry (Southwest University), Ministry of Education, College of Pharmaceutical Sciences, Southwest University, Chongqing, 400715, P. R. China.*

<sup>b</sup> *College of Chemistry and Chemical Engineering, Southwest University, Chongqing, 400715, P. R. China.*

*\*Corresponding author: [chengzhi@swu.edu.cn](mailto:chengzhi@swu.edu.cn)*

### Calculation of the energy level

The indirect band gap was calculated as described by Pankove<sup>1</sup> using the absorption measurements and the following equation.

$$\alpha h\nu = A(h\nu - E_g)^2 \quad (1)$$

Here  $\alpha$  is the absorption coefficient,  $A$  is a constant, and  $E_g$  is the indirect band gap of the semiconductor.

The potentials of VB and CB of a semiconductor material can be estimated according to the following empirical equations<sup>2</sup>:

$$E_{\text{VB}} = \chi - E^{\text{e}} + 0.5E_g \quad (2)$$

$$E_{\text{CB}} = E_{\text{VB}} - E_g \quad (3)$$

Wherein  $E_{\text{VB}}$  is the valence band edge potential,  $\chi$  is the electronegativity of the semiconductor, which is the geometric mean of the constituent atoms,  $E^{\text{e}}$  is the energy of free electrons on the hydrogen scale (about 4.5 eV vs NHE) and  $E_g$  is the band gap energy of the semiconductor. The  $E_{\text{VB}}$  of the  $\text{Cu}_{2-x}\text{Se}$  ( $x=0.26$ ) is -5.86 eV and the  $E_{\text{CB}}$  is -3.92 eV relative to vacuum potential.

For simpleness, HOMO/LUMO states of the TAMRA-DNA (-5.208 eV/-4.066 eV), AMCA (-6.407/-2.377 eV), Cy5 (-3.927/-3.482 eV) and pDA (-6.773eV/-5.045 eV) with quinone structure of DA can be calculated by B3LYP method respectively.

### Estimation of the molar extinction coefficient

The molar extinction coefficient of the as-prepared  $\text{Cu}_{2-x}\text{SeNPs}@p\text{DA}$  could be estimated from the experimentally measured absorbance values of various concentrations of NCs according to Lambert's law:

$$A(\lambda) = \varepsilon(\lambda)Lc \quad (4)$$

wherein  $A$  is the absorbance at the specific wavelength of  $\lambda$ ,  $\varepsilon$  is the molar extinction coefficient,  $L$  is the path length of the cuvette (1 cm), and  $c$  is the

concentration of nanocrystals in solution (mol L<sup>-1</sup>).

$$c = \frac{c_{wt,m}}{M_{NP}} = \frac{c_{wt,m}}{\frac{4}{3}\pi R^3 \rho N_A} \quad (5)$$

wherein  $c_{wt,m}$  is the weight concentration of the NPs (g L<sup>-1</sup>) measured according to freeze drying.  $M_{NP}$  is the molar weight of the nanocrystals (g mol<sup>-1</sup>),  $N_A$  is Avogadro's constant (mol<sup>-1</sup>), and  $R$  is the average radius of the spherical nanocrystals. The molar extinction coefficient of the as-prepared Cu<sub>2-x</sub>SeNPs@pDA can be calculated as  $2.6 \times 10^8$  M<sup>-1</sup>cm<sup>-1</sup>.

### The LSPR frequencies predicted with the classical Drude models

The localized surface plasmon resonance (LSPR) of Cu<sub>2-x</sub>SeNPs@pDA can be theoretically calculated by quasi-static approximation of Mie theory.<sup>3-5</sup> For spherical particles, the extinction cross section  $C_{ext}$  is given by,

$$C_{ext} = C_{abs} + C_{sca} = \frac{24\pi^2 R^3 \varepsilon_m^{3/2}}{\lambda} \frac{\varepsilon_2}{(\varepsilon_1 + 2\varepsilon_m)^2 + \varepsilon_2^2} \quad (6)$$

Wherein  $C_{abs}$  is the absorption cross section and  $C_{sca}$  is the scattering cross section,  $R$  is the particle radius,  $\varepsilon_m$  is the dielectric constant of the medium,  $\varepsilon_1$  and  $\varepsilon_2$  are the real part and imaginary part of the complex dielectric function  $\varepsilon = \varepsilon_1 + i\varepsilon_2$ , respectively,

which can be expressed by the Drude models,<sup>3</sup>

$$\varepsilon_1 = \varepsilon_\infty - \frac{\omega_p^2}{\omega^2 + \tau^2} \quad \varepsilon_2 = \frac{\omega_p^2 \tau}{(\omega^2 + \tau^2) \omega} \quad (7)$$

In which  $\omega_p$  is the bulk plasma frequency of Cu<sub>2-x</sub>SeNPs@pDA,  $\tau$  is the free carrier damping,  $\varepsilon_\infty$  is the high-energy dielectric constant and  $\omega$  is light frequency.

The free carrier density  $N$  can be got as follows,

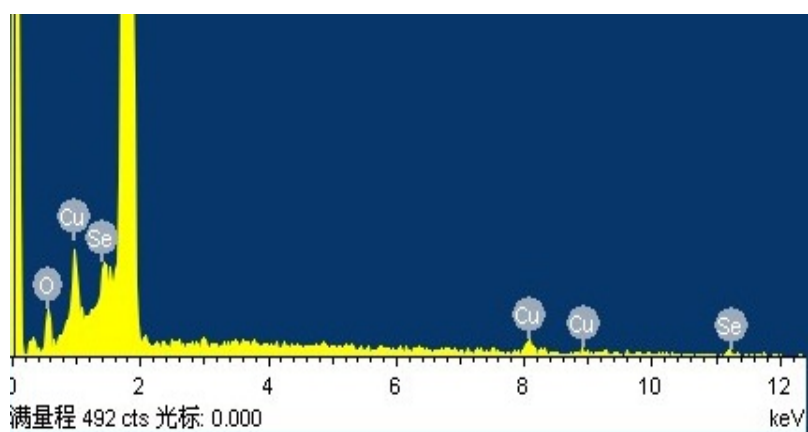
$$\omega_p^2 = \frac{Ne^2}{\varepsilon_0 m^*} \quad (8)$$

Wherein  $e$  is the elemental charge,  $\varepsilon_0$  is the free space permittivity, and  $m^*$  is the effective mass. As we could not find any report on the hole effective mass from the literature, a value of  $0.8m_0$  ( $m_0$  is the electron mass) was used in our calculation.<sup>6</sup> The  $\omega_F$  angular frequency can be calculated as  $9.13 \times 10^{15}$  rad s<sup>-1</sup> and Fermi wave-vector  $k$

is  $0.85 \times 10^8 \text{ cm}^{-1}$ .

**TABLE S1** Assay of the Nucleic Acid Sequence as Sensing Matrices

P1	5-TAMRA-CTG TCT TGA ACA TGA GTT-3
T1	5-AAC TCA TGT TCA AGA CAG-3
P2	5-TAMRA-AGT CCG TGG TAG GGC AGG TTG GGG TGA CT-3
Single-base mismatched (SBM) sequence for P1	5-AAC TCA TCT TCA AGA CAG-3
Noncomplementary (NC) sequence for P1	5-TTT CGC CTA CTT TTT GTT-3
P3	5-Cy5-CTG AAT TCT GGA TGT AGT-3
P4	5-AMCA-CTA GTT CTA AGT TCT GAT-3
T3	5-ACT ACA TCC AGA ATT CAG -3
T4	5-ATC AGA ACT TAG AAC TAG-3



Mean atom percent (%)		Stoichiometry
Cu	Se	
63.5	36.5	$\text{Cu}_{1.74}\text{Se}$

Figure S1. SEM-EDS spectrum of as prepared  $\text{Cu}_{2-x}\text{SeNPs}$ .

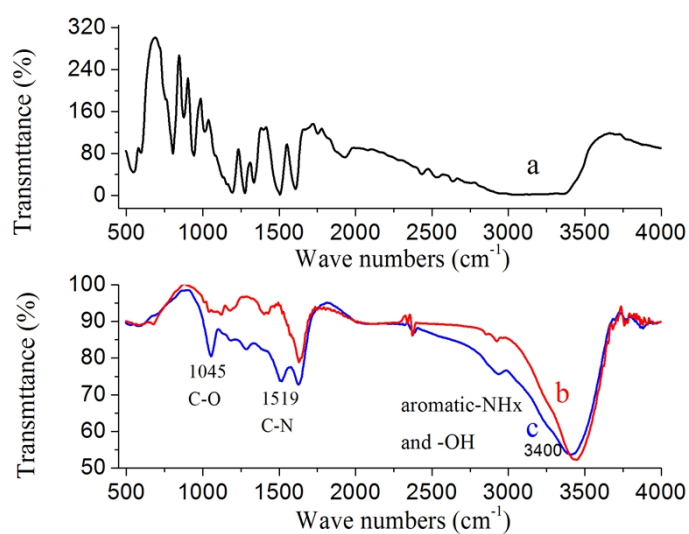


Figure S2. FTIR spectra of dopamine (a), Cu<sub>1.74</sub>SeNPs (b) and Cu<sub>1.74</sub>SeNPs@pDA (c). A broad peak around 3400 cm<sup>-1</sup> ascribed to aromatic -NHx and -OH stretching vibrations. The coatings also presented peaks at 1060 cm<sup>-1</sup> (C-O from vibrations benzene ring) and 1519 cm<sup>-1</sup> (N-H scissoring vibrations) which can be ascribed to the functional groups of dopamine.

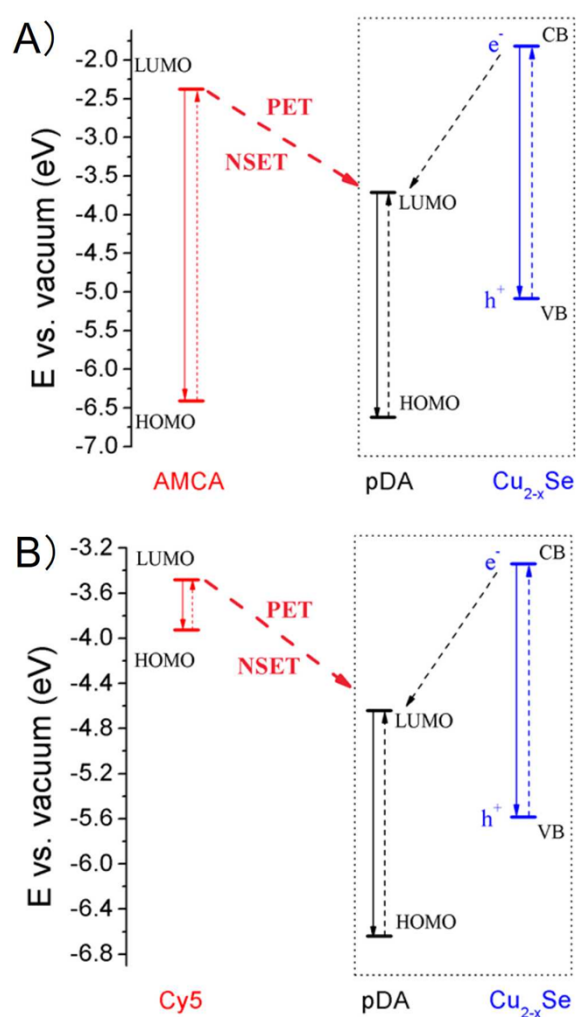


Figure S3 Schematic representation of Cu<sub>2-x</sub>Se conduction band (CB) and valence band (VB) relative to AMCA (A), Cy5 (B) and the quinone structure of DA and lowest unoccupied molecular orbital (LUMO) along with putative pathways for both the NSET and PET quenching pathways

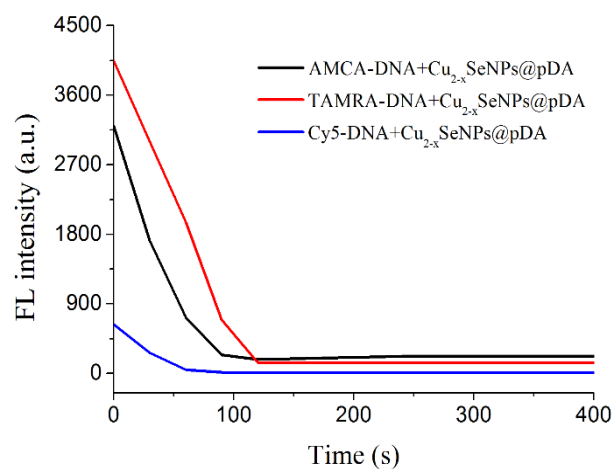


Figure S4. Fluorescence kinetics curves of 40 nM (TAMRA-DNA) P1, (Cy5-DNA) P3, and (AMCA-DNA) P4 upon addition of  $1.25 \text{ mg L}^{-1}$  of  $\text{Cu}_{2-x}\text{SeNPs@pDA}$ .

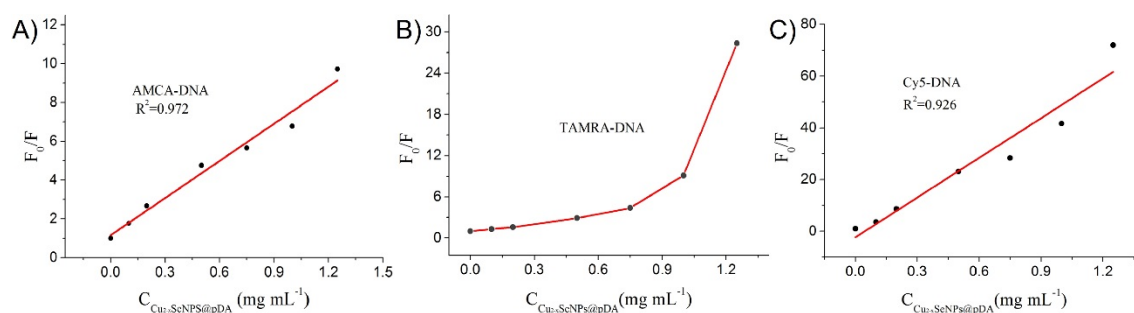


Figure S5. Stern–Volmer plots for 40 nM (A) AMCA-DNA, (B) TAMRA-DNA and (C) Cy5-DNA.  $F_0$  and  $F$  are the fluorescence intensity of the fluorophore in the absence and presence of  $\text{Cu}_{2-x}\text{SeNPs@pDA}$ , respectively.

**TABLE S2** Excited State Lifetimes Collected from Dyes-labelled DNA and Their Cu<sub>2-x</sub>SeNPs@pDA Conjugates

	Lifetime (ns)		
	$\tau_{av}$	$\tau_1$	$\tau_2$
AMCA-DNA	3.89	1.68 (24.81%)	4.62 (75.19%)
AMCA-DNA-Cu <sub>2-x</sub> SeNPs@pDA	0.58	0.39 (95.54)	4.61 (4.46%)
TAMRA-DNA	2.77	1.61 (39.08%)	3.52 (60.92%)
TAMRA-DNA-Cu <sub>2-x</sub> SeNPs@pDA	0.25	0.189 (97.26%)	2.56 (2.74%)
Cy5-DNA	1.57	0.937 (35.44%)	1.91 (64.56%)
Cy5-DNA-Cu <sub>2-x</sub> SeNPs@pDA	0.07	0.0322 (97.62)	1.63 (2.38%)

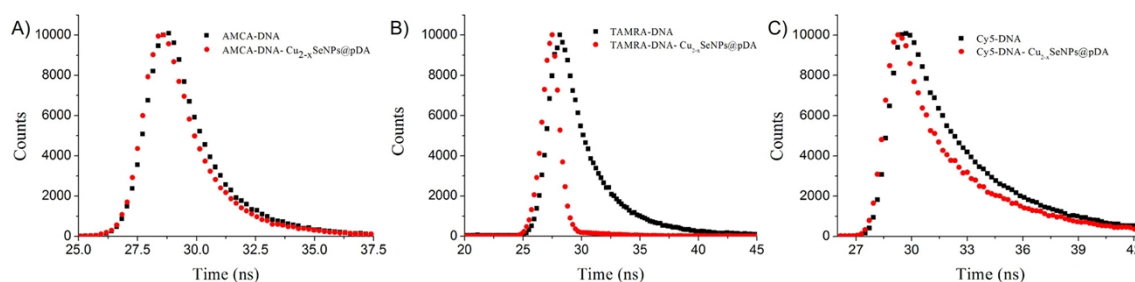


Figure S6. Time-resolved PL decays from the three dyes-labelled DNA donors.

**TABLE S3** Relevant Dyes-labelled DNA and Cu<sub>2-x</sub>SeNPs@pDA-dyes FRET and Photophysical Properties

Dyes	AMCA-DNA	TAMRA-DNA	Cy5-DNA
QY	0.49 <sup>7</sup>	0.68 <sup>8</sup>	0.25 <sup>9</sup>
Extinction coefficient of Cu <sub>2-x</sub> SeNPs@pDA (M <sup>-1</sup> cm <sup>-1</sup> )	2.6 × 10 <sup>8</sup>	2.6 × 10 <sup>8</sup>	2.6 × 10 <sup>8</sup>
Overlap integral J × 10 <sup>-10</sup> (cm <sup>3</sup> M <sup>-1</sup> )	6.25	8.60	15.1



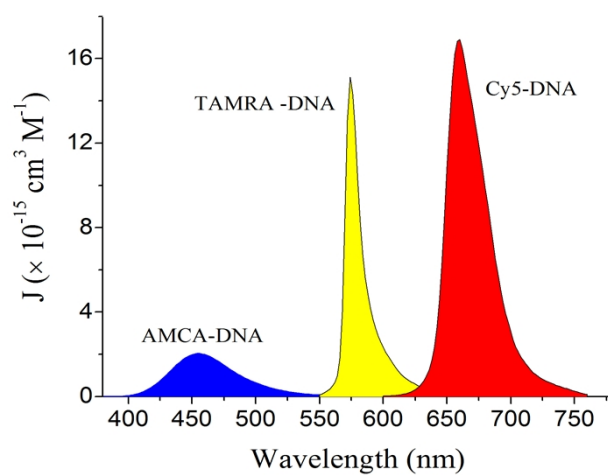


Figure S7. The spectral overlap function for each of the dyes-labelled DNA donors with the  $\text{Cu}_{2-x}\text{SeNPs}@p\text{DA}$  acceptor.

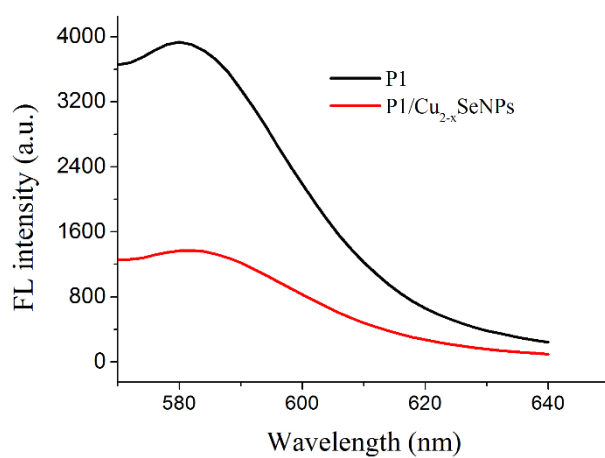


Figure S8. PL spectra collected from the emitting 40 nM P1 (TAMRA-labelled DNA) assembled with  $1.25 \text{ mg L}^{-1} \text{ Cu}_{2-x}\text{SeNPs}$  in PBS.

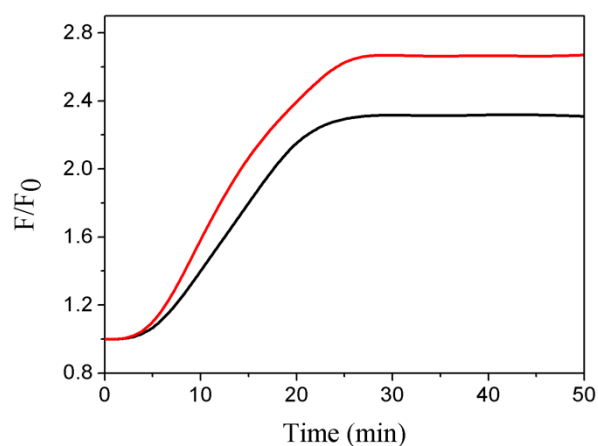


Figure S9. Fluorescence kinetics curves of P1/Cu<sub>2-x</sub>SeNPs@pDA upon addition of T1 (black line) and P2/Cu<sub>2-x</sub>SeNPs@pDA upon addition of thrombin.

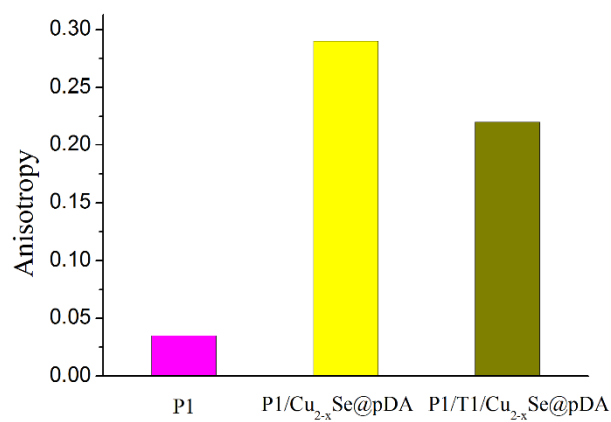


Figure S10. Fluorescence anisotropy of P1, P1/ Cu<sub>2-x</sub>SeNPs@pDA and P1/T1/ Cu<sub>2-x</sub>SeNPs@pDA with 40 nM P1 and 1.25 mg L<sup>-1</sup> Cu<sub>2-x</sub>SeNPs@pDA.

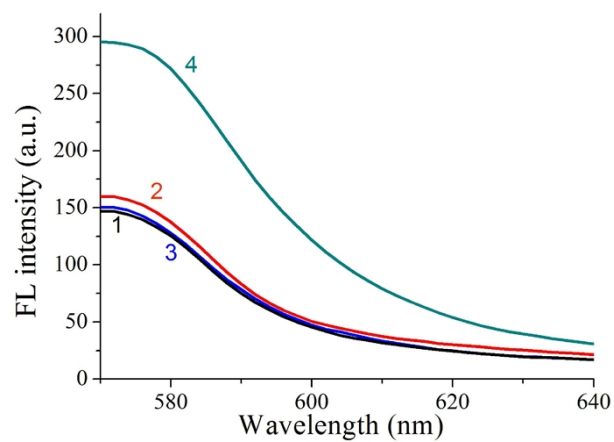


Figure S11. Fluorescence spectra of 40 nM P1-Cu<sub>2-x</sub>SeNPs@pDA (1) in the presence of 40 nM Single-base mismatched (SBM) sequence (2) , Noncomplementary (NC) sequence (3) and T1 (4).

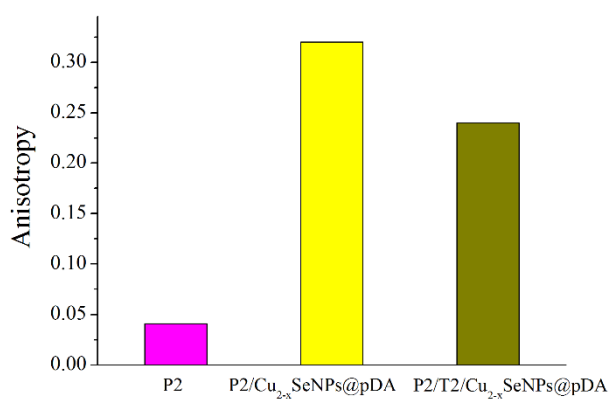


Figure S12. Fluorescence anisotropy of P2, P2/ Cu<sub>2-x</sub>SeNPs@pDA and P2/T2/ Cu<sub>2-x</sub>SeNPs@pDA with 60 nM P2 and 1.25 mg L<sup>-1</sup> Cu<sub>2-x</sub>SeNPs@pDA.

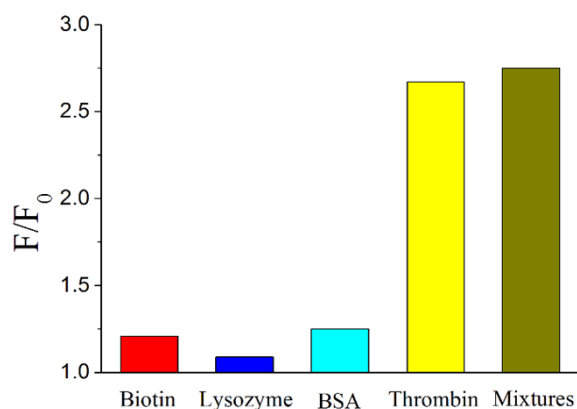


Figure S13. Specificity of the biosensing for thrombin over biotin, lysozyme, BSA and the mixtures (all at a concentration of 60 nM).

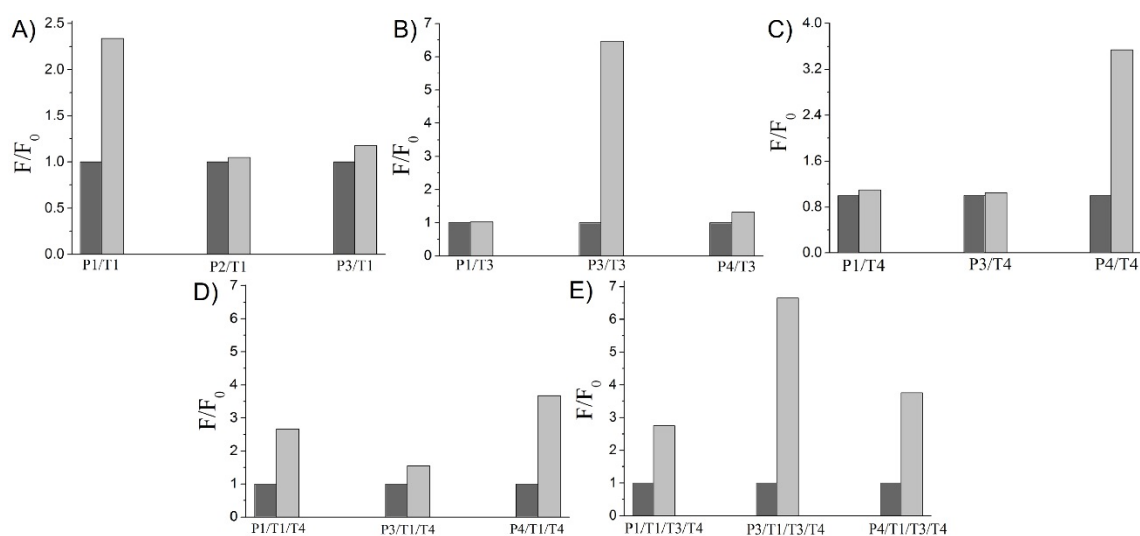


Figure S14. Multiplex and sequence-selective analysis of DNA. Three probes, P1, P3, and P4, labelled with TAMRA, Cy5, or AMCA, respectively, were individually excited at 540, 630, and 353 nm, emitting yellow (582nm), red (668 nm), and blue (452 nm) colors in these systems. The addition of target DNA (T1, T3, T4) of the corresponding dye-labelled DNA probe into the P1/P2/P3/Cu<sub>2-x</sub>SeNPs@pDA mixtures, resulting in significant fluorescence enhancement of the corresponding dyes at the respective P1, P3, P4 emitting channel.

## References

- 1 J. I. Pankove, *Optical Processes in Semi-Conductors*; Dover Publications: Mineola, NY, 1971.
- 2 Q. Li, H. Meng, P. Zhou, Y. Q. Zheng, J. Wang, J. G. Yu and J. R. Gong, *ACS Catal.*, 2013, **3**, 882-889.
- 3 J. M. Luther, P. K. Jain, T. Ewers and A. P. Alivisatos, *Nature Mater.*, 2011, **10**, 361.
- 4 F. Scotognella, G. Della Valle, A. R. S. Srimath Kandada, D. Dorfs, M. Zavelani-Rossi, M. Conforti, K. Miszta, A. Comin, K. Korobchevskaya, and G. Lanzani, *Nano Lett.*, 2011, **11**, 4711.
- 5 H. J. Yang, C. H. Chen, F. W. Yuan and H. Y. Tuan, *J. Phys. Chem. C*, 2013, **117**, 21955-21964.
- 6 Y. Xie, A. Riedinger, M. Prato, A. Casu, A. Genovese, P. Guardia, S. Sottini, C. Sangregorio, K. Miszta, S. Ghosh, T. Pellegrino and L. Manna, *J. Am. Chem. Soc.*, 2013, **135**, 17630.
- 7 K. F. Karlsson, P. A. J. S. Berg, K. P. R. Nilsson and O. Inganäs, *Chem. Mater.*, 2005, **17**, 4204.
- 8 <http://www.fluorophores.tugraz.at>.
- 9 M. P. Singh and G. F. Strouse, *J. Am. Chem. Soc.*, 2010, **132**, 9383.